# Comments on "The Impact of the Ice Phase and Radiation on a Midlatitude Squall Line System"

SCOTT A. BRAUN, ROBERT A. HOUZE JR., AND MING-JEN YANG

*Department of Atmospheric Sciences, University of Washington, Seattle, Washington*

17 August 1995 and 6 November 1995

ABSTRACT

This comment addresses two conclusions arising from a modeling study of Chin: that the contribution of mesoscale stratiform areas to large-scale heat and moisture budgets at midlatitudes is small compared to that associated with deep convection and that longwave radiative processes are the cause of the transition zone. A review of the literature and a comparison to another simulated squall line reaffirm the long-standing result that mesoscale stratiform precipitation regions often contribute significantly to the large-scale heating and moistening and demonstrate that longwave radiation is just one of the many factors that modify the kinematic and microphysical processes that form the transition zone.

## 1. Introduction

Mesoscale convective systems (MCSs) in the Tropics and in midlatitudes generally have regions of convective precipitation and adjacent or surrounding areas of lighter stratiform precipitation (Houze 1993, chapter 9). Observational studies conducted in the past two decades have demonstrated the importance of these precipitating convective and mesoscale stratiform regions of MCSs to budgets of heat, moisture, liquid water, and momentum (Leary and Houze 1980; Houze 1982; Gamache and Houze 1983; Johnson and Young 1983; LeMone 1983; Houze 1989; Chong and Hauser 1990; Gallus and Johnson 1991, 1992; Mapes 1993; Mapes and Houze 1995). Extensive nonprecipitating anvil clouds[1] associated with upper-level outflow from convective systems primarily affect the large-scale environment via heating budgets through their radiative feedbacks (Webster and Stephens 1980; Houze 1982). In a recent study, Chin (1994, hereafter referred to as C94) concluded that the stratiform precipitation and anvil regions of a midlatitude squall line made only minor contributions to the total heating and moistening of the large-scale environment based on the results of a numerical simulation.

Figure 1 shows a vertical structure representative of many mesoscale convective systems in both midlatitudes (Houze et al. 1990) and the Tropics (Zipser 1969; Houze 1977; Chong et al. 1987; Rasmussen and Rutledge 1993). The convective region contains intense, vertically oriented cores of radar reflectivity associated with strong vertical air motions. Rearward (relative to the direction of motion) of this convective region is a broad region of lighter, relatively uniform stratiform precipitation. Within the stratiform precipitation region is an area of enhanced radar reflectivity often called the *secondary maximum* or *secondary band.* Frequently, a minimum in the intensity of rain rate and radar reflectivity is located between the convective line and the secondary maximum of reflectivity in the stratiform precipitation region. This region is the *transition zone.* Several radar-based studies have investigated the causes of the secondary band and transition zone (Ligda 1956; Smull and Houze 1985; Rutledge and Houze 1987; Matejka and Schuur 1991; Biggerstaff and Houze 1993; Braun and Houze 1994a). C94 found that a transition zone formed only in a simulation that included longwave radiative processes and concluded that longwave radiation caused the transition zone.

C94 used a convective-cloud model to study the thermodynamic, microphysical, and radiative properties of a midlatitude broken-line squall line [the term "broken line" is based on the definition of Bluestein and Jain (1985, hereafter BJ)] and its impact on the large-scale environment. Although it may have been unintended, C94's statements regarding the thermodynamic impact of the stratiform precipitation region and the role of radiation in the formation of the transition zone implied that his results were general for midlatitude systems, particularly broken-line systems, and that longwave ra-

[1] These nonprecipitating clouds are referred to simply as anvils in the remainder of the text.

*Corresponding author address:* Dr. Scott A. Braun, National Center for Atmospheric Research, P.O. Box 3000, Boulder, CO 80307-3000.
E-mail: braun@ncar.ucar.edu

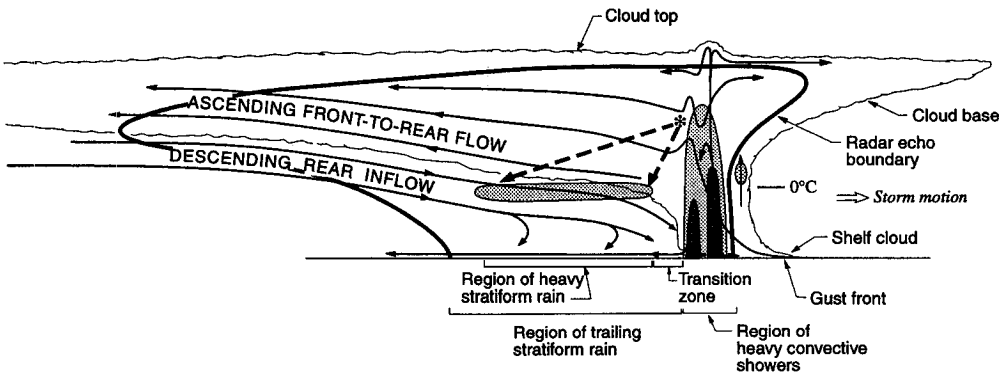


FIG. 1. Conceptual model of the kinematic, microphysical, and radar-echo structure of a convective line with trailing stratiform precipitation viewed in a vertical cross section oriented perpendicular to the convective line. Intermediate and strong radar reflectivity are indicated by medium and dark shading. (Adapted from Houze et al. 1989).

diation was the exclusive cause of the transition zone. This note demonstrates that the results of C94 are not general for midlatitude systems, including broken-line systems, primarily because of the comparatively small size of the stratiform precipitation region in his simulation. To make this point, in section 3 of this comment, we compare the simulated squall line of C94 to observed systems described in the literature and to a simulation (described in section 2) of a midlatitude broken-line squall line with a larger stratiform precipitation region by Yang and Houze (1995a, hereafter referred to as YH95). These comparisons reaffirm the longstanding result that mesoscale stratiform precipitation regions often contribute significantly to large-scale heating and moistening. In section 4, we further show that the transition zone develops primarily from kinematic and microphysical processes and that a wide range of factors (including radiation) affect these processes.

## 2. Description of the YH95 squall line simulation

To contrast C94's results with a simulation of another squall line, we use output from a high-resolution, nonhydrostatic numerical-model simulation of the 10–11 June 1985 PRE-STORM[2] squall line by YH95. This squall line is classifiable as a broken-line system, and a large-scale heat budget for this system (Gallus and Johnson 1991) was used by C94 to verify his simulation results. Our simulation was two-dimensional and included ice-phase microphysics. The Coriolis force, surface drag, and radiation were neglected. The horizontal resolution was 1 km within a 301-km-wide fine-mesh region, which was centered within a 4500-km-wide stretched grid. The ratio between adjacent grid points in the stretched mesh was 1.075:1. A three-dimensional simulation was similar to the two-dimensional simulation (YH95).

The initial thermodynamic and kinematic fields were specified from a sounding taken ahead of the 10–11 June squall line. This sounding was characterized by a convective available potential energy (CAPE) of 3323 J kg$^{-1}$, which is higher than the average value of 2820 J kg$^{-1}$ determined by BJ for springtime broken-line type squall lines. The initial line-normal wind profile is shown in Fig. 2 along with the wind profiles from BJ and C94. The YH95 wind profile is similar to that of BJ, but the magnitudes are shifted toward lower values; the magnitude of the vertical shear is somewhat stronger below 2 km and weaker above 5 km. The sharp decrease in velocity above 10 km in the YH95 profile is not apparent in the BJ profile, but it does not significantly affect the simulation results. The vertical shear in the 3–8 km layer in C94's profile is approximately 75% larger than that of BJ.

Convection was initiated by a 5-km deep, 170-km wide cold pool with a minimum potential temperature 6 K lower than the environmental air. See YH95 and Yang and Houze (1995b) for more details on the simulation and validation with observations. Since this simulation did not include radiative processes, direct comparisons are generally restricted to characteristics of the thermodynamic and microphysical fields of C94's no-radiation simulation with ice.

A time-averaged structure from the YH95 squall line simulation is shown in Fig. 3, which is a vertical cross section of half-hour-averaged hydrometeor fields for the mature stage [contours of rain (solid) and snow (dashed), shading of cloud water and ice]. The precipitation fields show an intense leading convective line ($x$ = 160 to 205 km) followed by a region of lighter

[2] Oklahoma–Kansas Preliminary Regional Experiment for the Storm-Scale Operational and Research Meteorology Program-Central Phase (Cunning 1986).

stratiform precipitation ($x \sim 50$ to 160 km). A secondary maximum of rain ($x = 75$ to 135 km) occurs within the stratiform precipitation region, and a transition zone (precipitation minimum) is between $x = 135$ to 160 km. The region behind the stratiform precipitation (the rear anvil region, $x < 50$ km) has no surface rainfall and only a little rain aloft. However, a substantial amount of precipitating ice remains aloft below a roughly 7-km thick cloud layer.

The simulated squall-line convective precipitation structures in C94 and YH95 are qualitatively similar. The fundamental difference between the simulations is in the horizontal extent of the stratiform precipitation region, which is significantly larger in YH95. The relevance of this difference is described in the next section. The size difference between the YH95 and C94 simulations may be related to the vertical wind shear above 3 km and the magnitude of the CAPE (which was 2742 J kg$^{-1}$ in C94). The stronger shear in C94 may produce a weaker upshear tilt or a downshear tilt of the convective line, which would weaken the front to rear flow and reduce the rearward transport of hydrometeors. In contrast, the weaker upper-level shear and higher CAPE in YH95 may result in a greater upshear tilt and stronger front to rear flow.

In the discussion below, we argue that the size of C94's simulated squall line is representative of the smaller end of the squall-line size spectrum (here size refers to the across-line width of the precipitation region). In contrast, the 10–11 June squall line simulated by YH95 is likely representative of the larger end of the size spectrum. The "true" (most representative) scale probably lies somewhere between these two cases. However, the scale of the 10–11 June squall line is typical of most major springtime rainstorms (Houze et al. 1990).

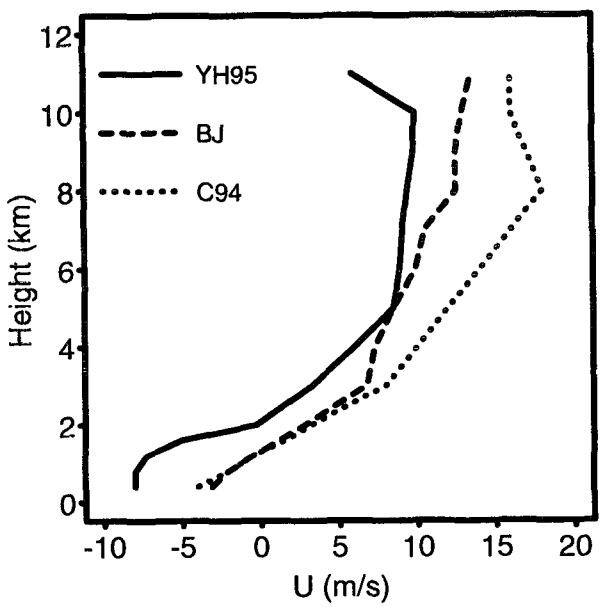


FIG. 2. Initial line-normal ground-relative wind profile for the simulation of YH95 (solid line). Also shown are the line-normal wind profile from Fig. 13a of BJ (dashed line) and the initial wind profile of C94 (dotted line).

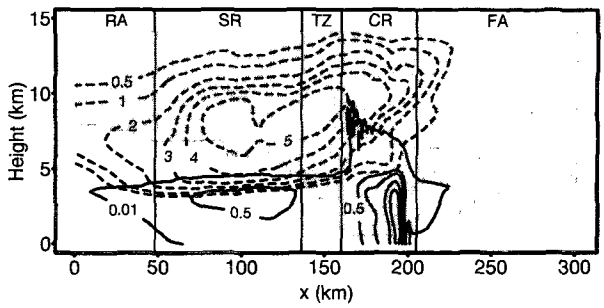


FIG. 3. Vertical cross section of rain (solid), precipitating ice (dashed), and cloud (water and ice, shaded). Contours are drawn at 1 g kg$^{-1}$ intervals with additional contours at 0.01 and 0.5 g kg$^{-1}$ for rain and 0.5 g kg$^{-1}$ for precipitating ice. Cloud water and ice mixing ratios greater than 0.01 g kg$^{-1}$ are shaded. Vertical lines separate the rear anvil (RA), stratiform precipitation region (SR), transition zone (TZ), convective region (CR), and forward anvil (FA). Based on the calculations of Yang and Houze (1995a).

## 3. The contribution of the stratiform precipitation and anvil regions to large-scale budgets

C94 computed vertical profiles of the apparent heating and moistening ($Q_1$ and $Q_2$) from model output and showed that for his squall line simulation the contributions of the stratiform precipitation and anvil regions to the total heating and drying were small compared to that of the convective region during the mature stage. Based on this one modeling case study, C94 concluded (and implied generality, at least for broken-line systems) that the thermodynamic feedbacks ($Q_1$ and $Q_2$) to large-scale systems at midlatitudes are dominated by the convective clouds and that the stratiform region contribution is small. We suggest that the generality of this conclusion, which is contrary to many previous studies, is limited to squall lines with small stratiform precipitation regions. Furthermore, as described below, the verification of the model $Q_1$ and $Q_2$ profiles against those of Gallus and Johnson (1991) is inappropriate.

Stratiform precipitation regions are important to budgets of heat and moisture in the Tropics (Leary and Houze 1980; Houze 1982, 1989; Johnson 1984; Johnson and Young 1983; Lafore et al. 1988; Chong and Hauser 1990; Tao et al. 1993). Only a small number of heat budget studies from observational data and model output with resolution sufficient to delineate the convective and stratiform components have been performed for midlatitudes (Gallus and Johnson 1991; Tao et al. 1993; Braun and Houze 1994b; Lin and Johnson

1994; C94).[3] Similar to the tropical studies, each of these midlatitude studies, with the exception of C94, shows a significant contribution of the stratiform precipitation region to the large-scale budgets of heat and moisture.

Since the magnitudes of vertical mass transports, and by implication diabatic heating, in stratiform precipitation regions tend to be similar among MCSs (Houze 1989), the importance of stratiform precipitation regions to heat and moisture budgets will generally be a strong function of the size of the stratiform precipitation areas. Houze and Cheng (1977) and Houze et al. (1990) showed that the size of stratiform radar echoes in MCSs can vary substantially from case to case. While the largest precipitation systems occur the least frequently (Houze 1993, chapter 9), they account for a large proportion of the warm-season rainfall in the central United States (Fritsch et al. 1986) and tend to be accompanied by large stratiform precipitation regions (Houze et al. 1990; McAnelly and Cotton 1992). In addition, Houze (1977), Churchill and Houze (1984), Houze and Rappaport (1984), Leary (1984), Wei and Houze (1987), and McAnelly and Cotton (1992) have shown that the stratiform area and stratiform contribution to rainfall increase with time in the lifecycle of MCSs. Thus, the impact of stratiform precipitation regions on heat and moisture budgets will tend to be maximum during the mature and dissipating stages of MCSs. Since C94's budget results are calculated for the mature stage only, his results do not reflect the increased contribution of the stratiform precipitation region during later stages.

For C94's simulation without radiation (see his Fig. 7f), the stratiform rainfall region spans only 20–60 km (the 0.01 g kg$^{-1}$ rain contour to the rear of the convective line spans only 20 km near the surface but 60 km near the 0°C level). These dimensions are very small compared to the sizes of many MCSs discussed in the literature that reach widths up to 100–200 km (Ogura and Liou 1980; Smull and Houze 1985, 1987; Leary and Rappaport 1987; Rutledge et al. 1988; Houze et al. 1990). The stratiform rain areas of such large systems contribute significantly to heat and moisture budgets. For example, in the midlatitude squall-line simulation of YH95, the stratiform rainfall region reached a width of approximately 90–150 km (the 0.01 g kg$^{-1}$ rain contour in Fig. 3 spans 90 km near the surface and 150 km near the 0°C level), which is somewhat less than the observed near-surface width of 120–150 km (Rutledge et al. 1988). Vertical profiles of latent heating rates[4] (Fig. 4) for the convective region and stratiform cloud (precipitating and nonprecipitating) region from the YH95 simulation show that the extensive stratiform region contributed significantly to the total heating and moistening of the large-scale environment. At upper levels, heating by condensation and deposition (Fig. 4) in the stratiform-cloud-region mesoscale ascent contributed significantly to the total heating. Below 4 km, the cooling by melting and evaporation in the stratiform cloud region generally exceeded the convective heating. Similar results were obtained from a dual-Doppler-derived heat budget for this squall line (Braun and Houze 1994b). The large stratiform contribution to the total heating in the case of the 10–11 June squall line, as indicated by both observations (Gallus and Johnson 1991; Braun and Houze 1994b) and modeling, suggests that C94's results likely apply only to systems accompanied by small stratiform precipitation regions.

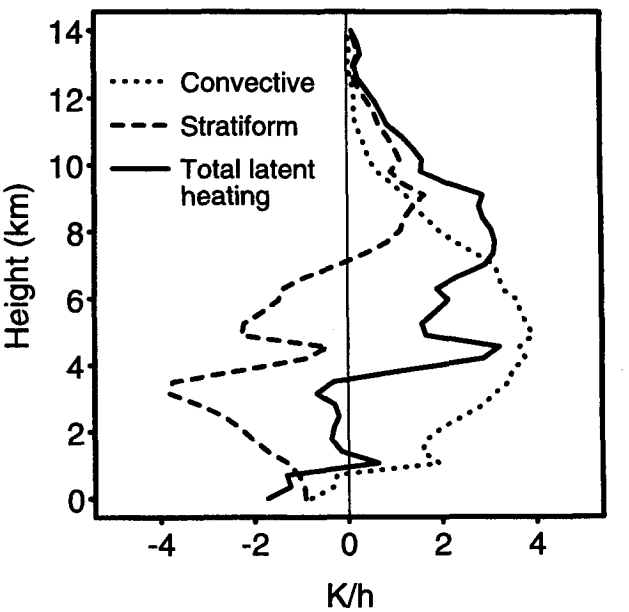


FIG. 4. Profiles of latent heating rates for the convective region, stratiform precipitation and anvil regions, and total (see Fig. 3). Based on the calculations of Yang and Houze (1995a).

Given that the size of the simulated stratiform precipitation region in C94 is small, one must ask whether this small size is representative of storms occurring in the specified environment (i.e., broken-line systems)

[3] The first three of these studies focused on the 10–11 June 1985 PRE-STORM squall line.

[4] Mean latent heating rates for the convective region and stratiform precipitation and nonprecipitating anvil regions were calculated by using a convective–stratiform separation technique identical to that of C94, except that a cloud water mixing ratio threshold of 0.1 g kg$^{-1}$ below the melting level is used instead of 0.2 g kg$^{-1}$ to identify developing, but nonprecipitating, convective cells. The separation technique is applied to instantaneous fields saved every two minutes for the half-hour period from which the average fields in Fig. 2 are obtained. In this analysis, we only consider data lying within the fine-mesh domain, which has boundaries at $x$ = 0 and 301 km.

or whether the model underestimates the size because of inappropriate model physics, the two-dimensionality constraint, or the increased wind shear in the 3–8-km layer (compared to BJ, Fig. 2) used by C94. Since the initial environment is specified by a composite sounding, no data from an individual storm are available for verification of the simulated storm structure or size in C94. Thus, the extent to which the size of the modeled storm in C94 represents the sizes of observed squall lines cannot be directly evaluated. In section 2, we suggested that the increased mid- to upper-level shear might suppress the strength of the front to rear flow and the size of the stratiform precipitation region.

The question of whether models underestimate the size of the stratiform precipitation region is not new. For example, in the simulations of the 10–11 June 1985 squall line by Tao et al. (1993) and YH95, the modeled stratiform surface rainfall regions extended only ~50 km (Tao et al. 1993, see their Fig. 2a) and 90 km (Fig. 3), respectively, to the rear of the convective line during the mature stage, compared to the observed width of 120–150 km. Fovell and Ogura (1988) suggested that the two-dimensionality constraint can underestimate the size of the stratiform precipitation region by limiting the production of condensate in the stratiform-region mesoscale ascent. C94 claims that the presence of a bright band in his simulation indicates that two-dimensionality was not a problem in his case. However, the presence of a bright band is irrelevant to the issue of the *size* of the stratiform precipitation region. Given the small size of the stratiform precipitation region and the lack of specific observations for verification, C94's claim that the two-dimensionality of the model did not limit the size of the stratiform precipitation region is unsupported. The model-derived radar reflectivity fields in Figs. 5 and 19 of C94 suggest that two-dimensionality, combined with dry low-level conditions (see Fig. 1 of C94), may have been a problem. In these figures, the reflectivity is seen to decrease very rapidly from greater than 35 dBZ near the melting level to less than 15 dBZ near 1 km. Such rapid decreases in reflectivity are not typically observed (Smull and Houze 1985; Leary and Houze 1979; Leary and Rappaport 1987; Rutledge et al. 1988; Schuur et al. 1991; Rasmussen and Rutledge 1993; Smull and Augustine 1993) and suggest that the two-dimensional assumption and the dry low-level initial conditions caused excessive erosion of the stratiform precipitation region from the rear. Further evidence that this type of erosion can be caused by the two-dimensionality of the model is provided in Fig. 3. The cloud water–ice field (shading) indicates subsaturated conditions in a relatively deep layer above the 0°C level (4.4 km) in the stratiform precipitation region. In contrast, observations for this case show nearly saturated conditions in the secondary band region above the 0°C level (Johnson and Hamilton 1988; Willis and Heymsfield 1989; Braun and Houze 1995). The drier conditions in the model are evidently caused by the fact that the dry air transported into the system by the rear inflow must be mixed in the convective and stratiform regions, whereas in a three-dimensional system this dry air can be transported in the along-line direction.

Two factors involving model microphysics may also contribute to the underestimation of the size of the stratiform precipitation region. The inclusion of hail throughout an entire simulation causes a significant amount of precipitating ice to fall out close to the convective region. It also reduces the amount of snow that is produced and, consequently, reduces the rearward transport of more slowly falling precipitation ice particles (Fovell and Ogura 1988; Yang and Houze 1995b). Houze et al. (1990) found that hail occurs primarily during the early stages of MCS growth, so the inclusion of hail beyond the early stages of a simulated storm may be unrealistic. An additional factor is the inclusion of density weighting in ice-particle fall speed formulas since this weighting may cause overestimates of the particle fall velocities at upper levels in bulk parameterization formulas (Braun and Houze 1994a). Yang and Houze (1995b) found that a much wider stratiform precipitation region was produced when the density weighting was removed.

Based on the profiles in Fig. 4 and on previous literature, we suggest that C94's conclusions regarding the small impact of the stratiform precipitation region on heating and moistening of the large-scale environment do not apply generally to midlatitude systems, including broken-line systems. It is uncertain whether the narrow stratiform region simulated in his study is a product of the initial environment, of the two-dimensionality constraint, or of deficiencies in the microphysical parameterization scheme. In any event, the narrow stratiform region in his study implies that his conclusions apply only to those systems that contain small stratiform precipitation regions, and as such they do not represent the storms accounting for the major precipitation events (Houze et al. 1990). They also do not represent the impact felt over the lifetime of the MCS.

One final concern is C94's comparison of the model-derived $Q_1$ and $Q_2$ profiles to the rawinsonde-based observational results of Gallus and Johnson (1991) to verify the model results. There is no reason to expect that the model-derived profiles should match the profiles of Gallus and Johnson (1991), which were obtained from the 10–11 June squall line. Profiles of $Q_1$ and $Q_2$ can vary substantially from case to case depending on environmental conditions, storm organization, and areas–amounts of convective versus stratiform precipitation. The structure of the modeled squall line does not compare well to that of the 10–11 June system since the stratiform precipitation region is much smaller than that of the 10–11 June storm (20–60 km wide versus 120–

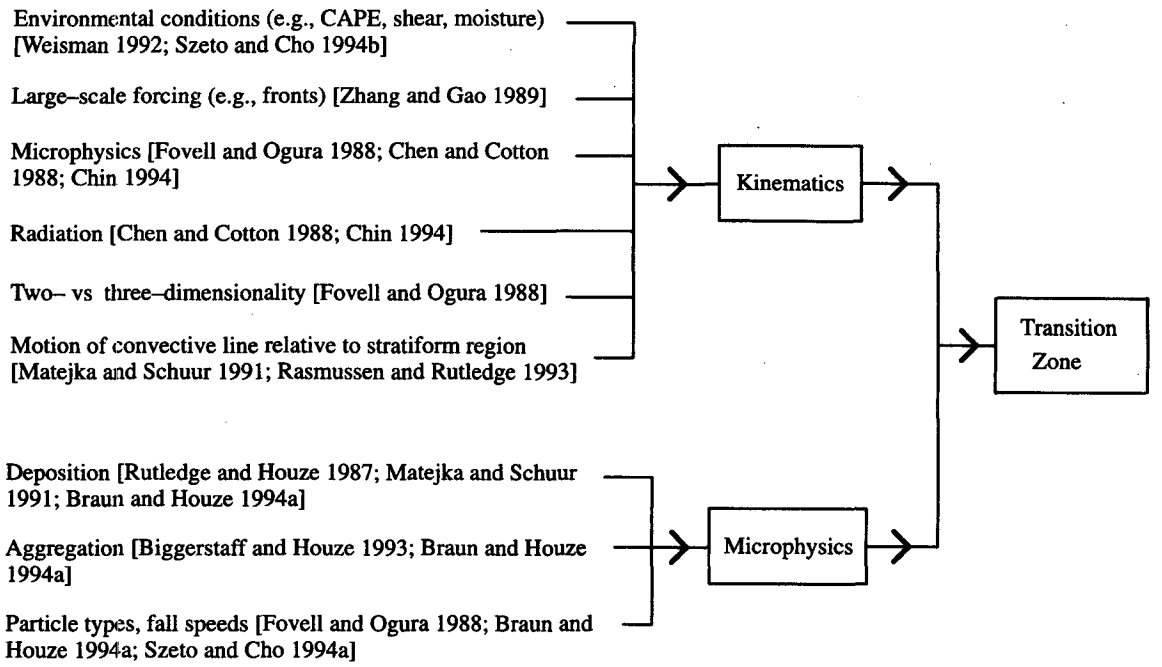


FIG. 5. Schematic diagram indicating factors important to the development of the transition zone. The transition zone is a direct result of the storm kinematics and microphysics. Any processes connected with the factors controlling the kinematics and/or microphysics can contribute to or hinder the formation of the transition zone but are not direct causes of the transition zone.

150 km). It would be a misinterpretation to suggest that the apparent agreement between C94's model results and Gallus and Johnson's (1991) diagnosed total heating rates leads to the conclusion that the total heating in the 10–11 June squall line was dominated by deep convection. This was not the case. The large stratiform precipitation area of the 10–11 June storm produced a very large stratiform component to the $Q_1$ and $Q_2$ profiles. Both the rawinsonde-based analysis of Gallus and Johnson (1991) and the radar-based budget of Braun and Houze (1994b), which has the resolution to delineate the convective and stratiform contributions, confirm the large contribution to $Q_1$ and $Q_2$ made by the stratiform precipitation region.

## 4. The transition zone

Before we discuss the mechanisms that are responsible for the formation of the transition zone reflectivity minimum, it is necessary that we define more precisely the term *transition zone.* We define the transition zone to be that region, in MCSs with leading line–trailing stratiform organization, of minimum radar reflectivity located below the 0°C level and between the leading convective line and the secondary maximum of radar reflectivity within the stratiform precipitation region. This region of minimum reflectivity is relatively steady (lasting a minimum of one hour). This definition of transition zone distinguishes it from regions of precipitation that are intermediary in time between convective and stratiform precipitation structure (Mapes and Houze 1993). Examples of well-defined transition zones include those seen in Ligda (1956), Smull and Houze (1985, 1987), Chong et al. (1987), Leary and Rappaport (1987), Schuur et al. (1991), Srivastava et al. (1986), and Biggerstaff and Houze (1993). Note that the existence of the transition zone depends inherently on the presence of the secondary maximum of radar reflectivity in the trailing stratiform region. Thus, the mechanisms that produce the transition zone include and may be dominated by those that cause the formation of the secondary band (Matejka and Schuur 1991; Biggerstaff and Houze 1993; Braun and Houze 1994a).

C94 found that a well-defined transition zone formed in his simulations only when longwave (but not shortwave) radiation was included. Consequently, C94 appears to conclude generally that longwave radiative processes *cause* the transition zone. However, Caniaux et al. (1994) have simulated a tropical squall line and Yang and Houze (1995a,b, see Fig. 3), and Szeto and Cho (1994) have simulated midlatitude squall lines with well-defined transition zones in the absence of radiative processes in the models. A review of recent literature (Rutledge and Houze 1987; Matejka and Schuur 1991; Biggerstaff and Houze 1993; Braun and Houze 1994a; Caniaux et al. 1994; Szeto and Cho 1994; C94) suggests that longwave radiation is just one

of many factors that can contribute to the formation of the transition zone. Below we present a brief synthesis of the results from these past studies.

Figure 5 shows a schematic diagram that summarizes the processes that contribute to the formation of the transition zone. Smull and Houze (1985), Rutledge and Houze (1987), Matejka and Schuur (1991), Biggerstaff and Houze (1991, 1993), and Braun and Houze (1994a) have shown that the transition zone and the secondary band result from the detrainment and rearward transport of convectively generated ice particles and their subsequent growth by vapor deposition and aggregation (Fig. 1). Although it has not been examined sufficiently, an additional cause of the transition zone may be the faster movement of the convective line relative to that of the trailing stratiform precipitation region (Matejka and Schuur 1991; Rasmussen and Rutledge 1993). If the convective line moves faster than the stratiform precipitation region, then an increasingly widening gap would be expected to form between the two regions. Thus, on the most fundamental level (and hence, directly connected to the transition zone in Fig. 5), the transition zone can be said to result from the combination of kinematic circulations and microphysical processes. This statement of cause and effect has the following implications: that all processes that affect the structure and strength of the mesoscale circulations or that modify the growth or distribution of precipitating particles can affect the development of the transition zone. Some of the important processes described in the literature are shown in Fig. 5 (not necessarily in order of importance). Thus, these processes (longwave radiative processes among them) can contribute to or hinder the development of the transition zone but should not be ascribed as direct *causes* of the transition zone—certainly not the exclusive cause.

Causal relationships based on sensitivity tests with models must be made with caution. Adjustment or inclusion of a physical parameter or process in simulations of convective systems can indicate sensitivity of the physical system to that process but does not necessarily imply causality. If, in a highly nonlinear physical system, one parameter is changed and a new result is obtained, it cannot be concluded that the change of the parameter was the approximate cause of the new result.

## 5. Summary

In this comment, we address two questions arising from C94. The first is C94's conclusion that the contribution of mesoscale stratiform cloud areas (precipitating and nonprecipitating) to large-scale heat and moisture budgets is small compared to that associated with deep convection. We suggest that this conclusion applies only to convective systems with small stratiform precipitation areas (in his case, only 20–60 km wide). Houze et al. (1990) showed that the major precipitation events in Oklahoma in the spring, that is, the storms that dominate the total latent heat release, always in fact have a large component of stratiform precipitation. Observational case studies and budget studies in the literature show that it is primarily the size of the stratiform precipitation area that generally determines the magnitude of the stratiform contribution to large-scale feedback. Since the sizes of stratiform precipitation areas vary considerably in MCSs, so too do their contributions to the feedback to larger scales. In addition, the magnitude of the stratiform-region feedback relative to that of deep convection varies within the lifetime of a given MCS and is generally maximum in the dissipating stage.

The second question concerns the mechanisms that lead to the formation of the transition zone in squall lines with leading line–trailing stratiform structure. Based on simulations with and without longwave radiation in which a transition zone formed only in the presence of longwave radiation, C94 concluded that longwave radiative processes *caused* the formation of the transition zone. A review of the literature reveals that the transition zone is fundamentally a product of the kinematics and microphysical processes within the squall line. Any process (including longwave radiation) that can affect the kinematics (as in C94) or the microphysical processes can contribute to or hinder the development of the transition zone. However, such processes should not be ascribed as direct causes of the transition zone.

*Acknowledgments.* We thank Sandra Yuter and the three anonymous reviewers for their comments on the manuscript. G. C. Gudmundson edited the manuscript and Kay Dewar helped draft the figures. This research was sponsored by National Science Foundation Grant ATM-9409988.

## REFERENCES

Biggerstaff, M. I., and R. A. Houze Jr., 1991: Kinematic and precipitation structure of the 10–11 June 1985 squall line. *Mon. Wea. Rev.*, **119,** 3034–3065.

——, and ——, 1993: Kinematics and microphysics of the transition zone of the 10–11 June 1985 squall line. *J. Atmos. Sci.*, **50,** 3091–3110.

Bluestein, H. B., and M. H. Jain, 1985: Formation of mesoscale lines of precipitation: Severe squall lines over Oklahoma during the spring. *J. Atmos. Sci.*, **42,** 1711–1732.

Braun, S. A., and R. A. Houze Jr., 1994a: The transition zone and secondary maximum of radar reflectivity behind a midlatitude squall line: Results retrieved from Doppler radar data. *J. Atmos. Sci.*, **51,** 2733–2755.

——, and ——, 1994b: The heat and potential vorticity budgets of a midlatitude squall line. Preprints, *Sixth Conf. on Mesoscale Processes,* Portland, OR, Amer. Meteor. Soc., 335–338.

——, and ——, 1995: Melting and freezing in a mesoscale convective system. *Quart. J. Roy. Meteor. Soc.*, **121,** 55–77.

Caniaux, G., J.-L. Redelsperger, and J.-P. Lafore, 1994: A numerical study of the stratiform region of a fast-moving squall line. Part

I: General description and water and heat budgets. *J. Atmos. Sci.*, **51**, 2046–2074.

Chen, S., and W. R. Cotton, 1988: The sensitivity of a simulated extratropical mesoscale convective system to longwave radiation and ice phase microphysics. *J. Atmos. Sci.*, **45**, 3897–3910.

Chin, H.-N. S., 1994: The impact of the ice phase and radiation on a midlatitude squall line system. *J. Atmos. Sci.*, **51**, 3320–3343.

Chong, M.-D., and D. Hauser, 1990: A tropical squall line observed during the COPT81 experiment in West Africa. Part III: Heat and moisture budgets. *Mon. Wea. Rev.*, **118**, 1696–1706.

——, A. G. Scialom, and J. Testud, 1987: A tropical squall line observed during the COPT81 experiment in West Africa. Part I: Kinematic structure inferred from dual-Doppler radar data. *Mon. Wea. Rev.*, **115**, 670–694.

Churchill, D. D., and R. A. Houze Jr., 1984: Development and structure of winter monsoon cloud clusters on 10 December 1978. *J. Atmos. Sci.*, **41**, 933–959.

Cunning, J. B., 1986: The Oklahoma–Kansas Preliminary Regional Experiment for STORM–Central. *Bull. Amer. Meteor. Soc.*, **67**, 1478–1486.

Fovell, R. G., and Y. Ogura, 1988: Numerical simulation of a midlatitude squall line in two dimensions. *J. Atmos. Sci.*, **45**, 3846–3879.

Fritsch, J. M., R. J. Kane, and C. R. Chelius, 1986: The contribution of mesoscale convective weather systems to the warm-season precipitation in the United States. *J. Climate Appl. Meteor.*, **25**, 1333–1345.

Gallus, W. A., Jr., and R. H. Johnson, 1991: Heat and moisture budgets of an intense midlatitude squall line. *J. Atmos. Sci.*, **48**, 122–146.

——, and ——, 1992: The momentum budget of an intense midlatitude squall line. *J. Atmos. Sci.*, **49**, 422–450.

Gamache, J. F., and R. A. Houze Jr., 1983: Water budget of a mesoscale convective system in the tropics. *J. Atmos. Sci.*, **40**, 1835–1850.

Houze, R. A., Jr., 1977: Structure and dynamics of a tropical squall line system. *Mon. Wea. Rev.*, **105**, 1540–1567.

——, 1982: Cloud clusters and large-scale vertical motions in the Tropics. *J. Meteor. Soc. Japan*, **60**, 396–410.

——, 1989: Observed structure of mesoscale convective systems and implications for large-scale heating. *Quart. J. Roy. Meteor. Soc.*, **115**, 424–461.

——, 1993: *Cloud Dynamics.* Academic Press, 573 pp.

——, and C.-P. Cheng, 1977: Radar characteristics of tropical convection observed during GATE: Mean properties and trends over the summer season. *Mon. Wea. Rev.*, **105**, 964–980.

——, and E. N. Rappaport, 1984: Air motions and precipitation structure of an early summer squall line over the eastern tropical Atlantic. *J. Atmos. Sci.*, **41**, 553–574.

——, S. A. Rutledge, M. I. Biggerstaff, and B. F. Smull, 1989: Interpretation of Doppler weather radar displays in midlatitude mesoscale convective systems. *Bull. Amer. Meteor. Soc.*, **70**, 608–619.

——, B. F. Smull, and P. Dodge, 1990: Mesoscale organization of springtime rainstorms in Oklahoma. *Mon. Wea. Rev.*, **118**, 613–654.

Johnson, R. H., 1984: Partitioning tropical heat and moisture budgets into cumulus and mesoscale components: Implications for cumulus parameterization. *Mon. Wea. Rev.*, **112**, 1590–1601.

——, and G. S. Young, 1983: Heat and moisture budgets of tropical mesoscale anvil clouds. *J. Atmos. Sci.*, **40**, 2138–2147.

——, and P. J. Hamilton, 1988: The relationship of surface pressure features to the precipitation and airflow structure of an intense midlatitude squall line. *Mon. Wea. Rev.*, **116**, 1444–1472.

Lafore, J.-P., J.-L. Redelsperger, and G. Jaubert, 1988: Comparison between a three-dimensional simulation and Doppler radar data of a tropical squall line: Transport of mass, momentum, heat, and moisture. *J. Atmos. Sci.*, **45**, 3483–3500.

Leary, C. A., 1984: Precipitation structure of the cloud clusters in a tropical easterly wave. *Mon. Wea. Rev.*, **112**, 313–325.

——, and R. A. Houze Jr., 1979: Melting and evaporation of hydrometeors in precipitation from anvil clouds of deep tropical convection. *J. Atmos. Sci.*, **36**, 669–679.

——, and ——, 1980: The contribution of mesoscale motions to the mass and heat fluxes of an intense tropical convective system. *J. Atmos. Sci.*, **37**, 784–796.

——, and E. N. Rappaport, 1987: The life cycle and internal structure of a mesoscale convective complex. *Mon. Wea. Rev.*, **115**, 1503–1527.

LeMone, M. A., 1983: Momentum transport by a line of cumulonimbus. *J. Atmos. Sci.*, **40**, 1815–1834.

Ligda, M. G. H., 1956: The radar observations of mature prefrontal squall lines in the midwestern United States. *VI Congress of Organisation Scientifique et Technique Internationale du Vol a Voile (OSTIV)*, St-Yan, France, Aeronautical International Federation, 1–3.

Lin, X., and R. H. Johnson, 1994: Heat and moisture budgets and circulation characteristics of a frontal squall line. *J. Atmos. Sci.*, **51**, 1661–1681.

Mapes, B., 1993: Gregarious tropical convection. *J. Atmos. Sci.*, **50**, 2026–2037.

——, and R. A. Houze Jr., 1993: An integrated view of the 1987 Australian monsoon and its mesoscale convective systems. Part II: Vertical structure. *Quart. J. Roy. Meteor. Soc.*, **119**, 733–754.

——, and ——, 1995: Diabatic divergence profiles in western Pacific mesoscale convective systems. *J. Atmos. Sci.*, **52**, 1807–1828.

Matejka, T., and T. J. Schuur, 1991: The relationship between vertical air motions and the precipitation band in the stratiform region of a squall line. Preprints, *25th Conf. on Radar Meteorology*, Paris, France, Amer. Meteor. Soc., 501–504.

McAnelly, R. L., and W. R. Cotton, 1992: Early growth of mesoscale convective complexes: A meso-$\beta$-scale cycle of convective precipitation? *Mon. Wea. Rev.*, **120**, 1851–1877.

Ogura, Y., and M. T. Liou, 1980: The structure of a midlatitude squall line. A case study. *J. Atmos. Sci.*, **37**, 553–567.

Rasmussen, E. N., and S. A. Rutledge, 1993: Evolution of quasi-two-dimensional squall lines. Part I: Kinematic and reflectivity structure. *J. Atmos. Sci.*, **50**, 2584–2606.

Rutledge, S. A., and R. A. Houze Jr., 1987: A diagnostic modeling study of the trailing stratiform region of a midlatitude squall line. *J. Atmos. Sci.*, **44**, 2640–2656.

——, ——, M. I. Biggerstaff, and T. Matejka, 1988: The Oklahoma–Kansas mesoscale convective system of 10–11 June 1985: Precipitation structure and single-Doppler radar analysis. *Mon. Wea. Rev.*, **116**, 1409–1430.

Schuur, T. J., B. F. Smull, W. D. Rust, and T. C. Marshall, 1991: Electrical and kinematic structure of the stratiform precipitation region trailing an Oklahoma squall line. *J. Atmos. Sci.*, **48**, 825–842.

Smull, B. F., and R. A. Houze Jr., 1985: A midlatitude squall line with a trailing region of stratiform rain: Radar and satellite observations. *Mon. Wea. Rev.*, **113**, 117–133.

——, and ——, 1987: Dual-Doppler radar analysis of a midlatitude squall line with a trailing region of stratiform rain. *J. Atmos. Sci.*, **44**, 2128–2148.

——, and J. A. Augustine, 1993: Multiscale analysis of a mature mesoscale convective complex. *Mon. Wea. Rev.*, **121**, 103–132.

Srivastava, R. C., T. J. Matejka, and T. J. Lorello, 1986: Doppler radar study of the trailing-anvil region associated with a squall line. *J. Atmos. Sci.*, **43**, 356–377.

Szeto, K. K., and H.-R. Cho, 1994: A numerical investigation of squall lines. Part I. The control experiment. *J. Atmos. Sci.,* **51,** 414–424.

Tao, W.-K., J. Simpson, C.-H. Sui, B. Ferrier, S. Lang, J. Scala, M.-D. Chou, and K. Pickering, 1993: Heating, moisture, and water budgets of tropical and midlatitude squall lines: Comparisons and sensitivity to longwave radiation. *J. Atmos. Sci.,* **50,** 673–690.

Webster, P. J., and G. L. Stephens, 1980: Tropical upper-tropospheric extended clouds: Inferences from Winter MONEX. *J. Atmos. Sci.,* **37,** 1521–1541.

Wei, T., and R. A. Houze Jr., 1987: The GATE squall line of 9–10 August 1974. *Adv. Atmos. Sci.,* **4,** 85–92.

Weisman, M. L., 1992: The role of convectively generated rear-inflow jets in the evolution of long-lived mesoconvective systems. *J. Atmos. Sci.,* **49,** 1826–1847.

Willis, P. T., and A. J. Heymsfield, 1989: Structure of the melting layer in mesoscale convective system stratiform precipitation. *J. Atmos. Sci.,* **46,** 2008–2025.

Yang, M.-J., and R. A. Houze Jr., 1995a: Multicell squall line structure as a manifestation of vertically trapped gravity waves. *Mon. Wea. Rev.,* **123,** 641–661.

——, and ——, 1995b: Sensitivity of squall line rear inflow to ice microphysics and environmental humidity. *Mon. Wea. Rev.,* **123,** 3175–3193.

Zhang, D.-L., and K. Gao, 1989: Numerical simulation of an intense squall line during 10–11 June 1985 PRE-STORM. Part II: Rear inflow, surface pressure perturbations, and stratiform precipitation. *Mon. Wea. Rev.,* **117,** 2067–2094.

Zipser, E. J., 1969: The role of organized unsaturated convective downdrafts in the structure and rapid decay of an equatorial disturbance. *J. Appl. Meteor.,* **8,** 799–814.